

Low-Angle Synchrotron Radiation Diffraction with Glass-Capillary Optics

P. Engström and C. Riekkel

European Synchrotron Radiation Facility, BP 220, F-38043 Grenoble CEDEX, France

(Received 19 December 1995; accepted 30 January 1996)

The use of borosilicate-glass-capillary optics at a chosen wavelength for low scattering has been explored using an undulator beam at the ESRF. With a 2.3 μm beam at 0.092 nm wavelength, a silver behenate powder sample was scanned in two dimensions with a 2 μm step width. Scattering from single crystallites with $d_{001} = 5.83$ nm could be observed. The limit for observation, at low angles, was $ca\ s \simeq 0.1\ \text{nm}^{-1}$ ($s = 1/d$ for $d \simeq 10$ nm).

Keywords: glass-capillary optics; low-angle scattering; microfocus; undulator focusing; WAXS/SAXS instrumentation.

1. Introduction

Glass-capillary optics based on a polychromatic beam have been used at several second-generation synchrotron radiation sources in order to generate beam sizes down to the sub-micrometer range (see *e.g.* Engström, 1991; Bilderback, Thiel, Pahl & Brister, 1994). Applications reported in monochromatic diffraction using an undulator insertion device have been limited to wide-angle scattering with beam sizes down to a few micrometers (Engström, Fiedler & Riekkel, 1995; Riekkel & Engström, 1995). The low scattering background of an $\sim 2\ \mu\text{m}$ glass capillary around the primary beam had, however, already been noted (Engström, Riekkel & Chanzy, 1995). This communication aims at determining a practical limit to the minimum scattering vector s_{min} attainable by glass-capillary optics. Small s values are, for example, of interest for applications in fibre diffraction.

2. Capillary optics

As in other total reflection optics, the use of glass-capillary optics is based on the reflectivity curve which has its angular maximum at a critical angle (θ_c). By increasing the electron density of the surface layer (increase of atomic number, Z), θ_c , and hence the energy range, can be increased. However, the reflectivity below θ_c is higher for a low- Z than for a high- Z material due to absorption. For a mirror, one is usually using only one reflection so that the shape of the reflectivity curve is not so important. For glass-capillary optics, however, where the extreme number of reflections can be of the order of 100, not only θ_c but also the shape of the reflectivity curve will play a role. Thus, lead glass has about two times higher θ_c and a higher absorption than borosilicate glass. For many cases, therefore, the borosilicate glass is better to use.

The probability for an X-ray to pass through a borosilicate capillary is high if the angle of incidence for the last reflection stays below θ_c . The maximum gain factor for flux-density increase (I_g) can be written as

$$I_g = \theta_c^2 / 2.35 \sigma'_x \sigma'_z$$

assuming unit reflectivity (Thiel, Stern, Bilderback & Lewis, 1989). σ'_x and σ'_z are the source divergences in the horizontal and vertical planes.

In order to obtain a high gain for glass-capillary optics the direct beam from an undulator could be used, but the acceptance of a tapered glass capillary with an exit beam size of 1–2 μm is only $ca\ 50\ \mu\text{m}$. Another way to obtain a high flux density is to use a focusing mirror that accepts the full beam and to use a glass capillary for post-condensing of the beam. This option has been chosen in the present case.

3. Experimental

At the ESRF microfocus beamline the full beam of 7.5 (h) \times 0.8 (v) mm^2 is focused by an ellipsoidal mirror to a spot of 20 (h) \times 40 (v) μm^2 (full width at half maximum, FWHM) with a divergence of the order of 2.4 (h) \times 0.3 (v) mrad^2 (FWHM) (Engström, Fiedler & Riekkel, 1995). This focal spot with its size and divergence will act as a source for the glass capillary.

Experiments were performed at 13 keV ($\lambda = 0.092$ nm) which gives $\theta_c = 2.3$ mrad for borosilicate-glass capillaries. The expected gain factor in this case cannot exceed 7.5; the measured value gives 4. Capillaries were aligned using a motorized gimbal system together with an X-ray video camera. The sample was placed on an x/y translation stage within $\leq 500\ \mu\text{m}$ of the capillary exit. A 2.4 m long evacuated beamtube with a 160 mm diameter Kapton exit window was installed between sample and detector (Fig. 1).

The beamstop was located in the vacuum tube close to the exit window.

Both image plate (Molecular Dynamics) and an image-intensified X-ray video camera (Photonic Science) were

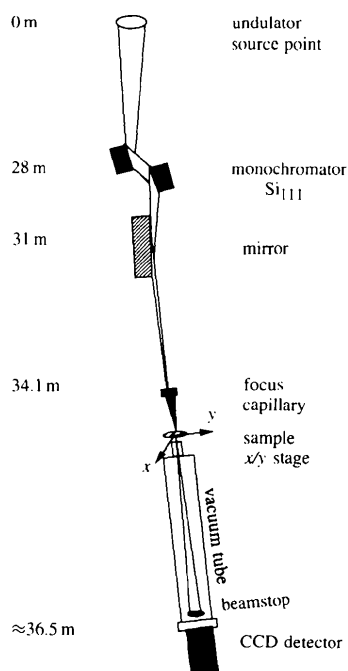


Figure 1
Schematic design of the experimental set-up (side view).

used. Images obtained with the image-intensified camera were corrected for distortion using the software package *FIT2D* (Hammersley, 1995; Hammersley, Svensson & Thompson, 1994)

Low-angle diffraction experiments were performed on a powder sample of silver behenate [$\text{CH}_3(\text{CH}_2)_{20}\text{CO}_2\text{Ag}$] which has been proposed as a low-angle scattering standard based on a synchrotron radiation study (Huang, Toraya, Blanton & Wu, 1993). The long spacing was determined as $d_{001} = 5.8380(3) \text{ nm}$.

4. Results and discussion

Fig. 2 shows the results of a two-dimensional scan with a $2.3 \mu\text{m}$ beam (full width) of the silver behenate powder sample with a step size of $2 \mu\text{m}$ between individual frames. Each frame was accumulated for 24 s. In order to mask the direct beam, a $26 \times 26 \text{ mm}^2$ beamstop was necessary while the expected direct beam size diameter was 11 mm. This shows the presence of additional scattering around the primary beam. Of the capillaries, the $2.3 \mu\text{m}$ glass capillary showed the least scattering around the primary beam which suggests an influence of fabrication tolerances on the background scattering. In principle it might be possible to reduce this scattering further by an aperture at the capillary exit although the sample would then move further away from the capillary exit resulting in a larger beam diameter.

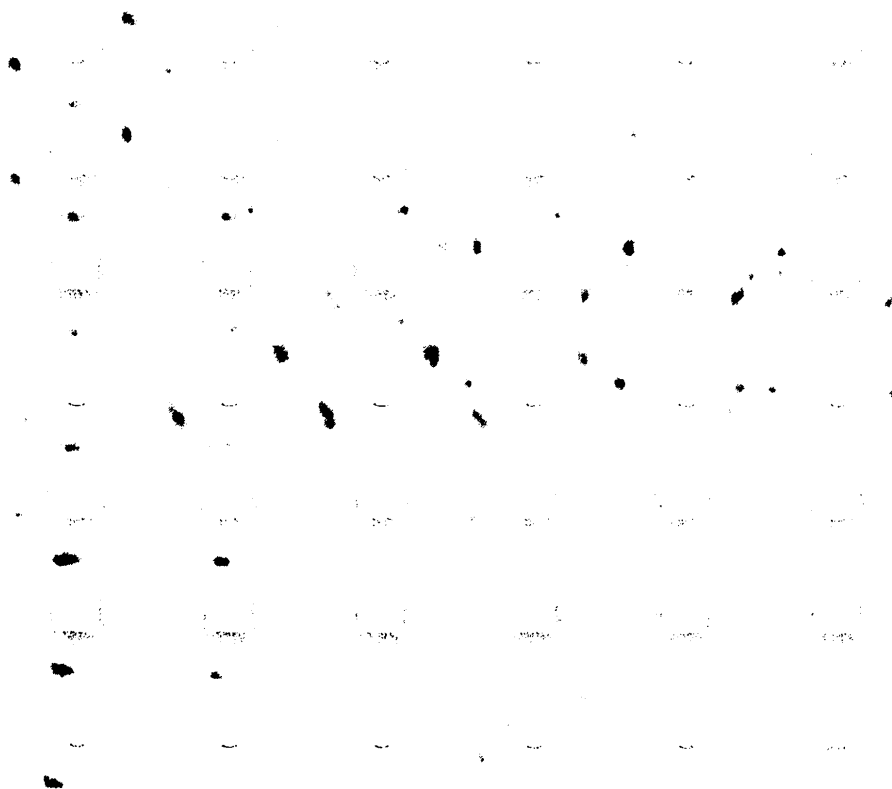
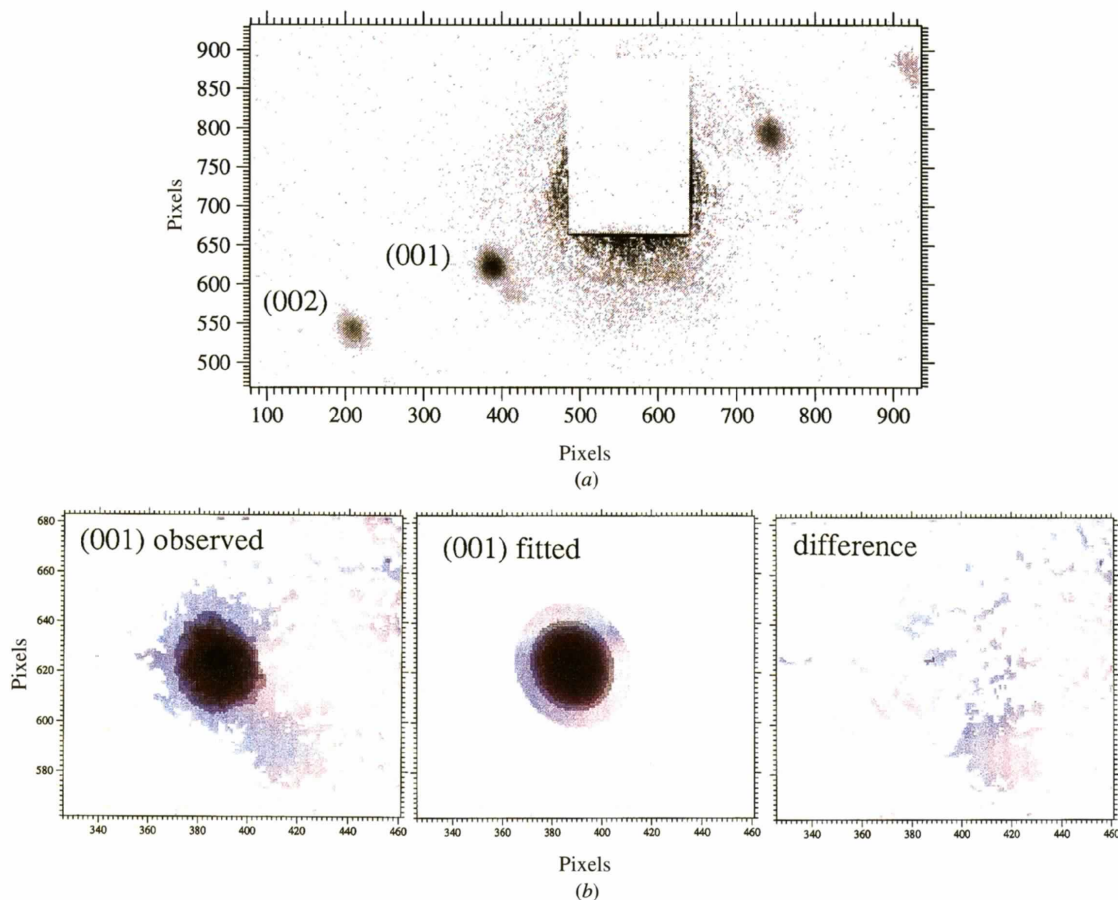
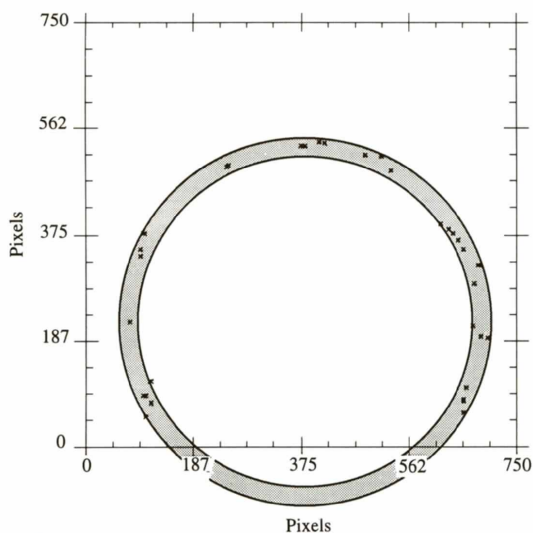


Figure 2
Successive images in a two-dimensional scan with $2 \mu\text{m}$ scan width of a silver behenate powder. The beam size is $2 \mu\text{m}$. Image-intensified camera (pixel size $121 \mu\text{m}$), background subtracted.

**Figure 3**

(a) Pattern showing a single silver behenate crystallite with weak scattering of a second crystallite; image plate (pixel size $200\ \mu\text{m}$), background subtracted. (b) Left: observed (001) reflection [note the weak second (001) reflection]; middle: two-dimensional Gaussian fit of (001) reflection; right: difference observed – fitted profile.

**Figure 4**

Peak positions of (001) reflections observed in Fig. 2.

Part of the frames in Fig. 2 show the (001) reflection of silver behenate. While in most cases two or more crystallites seem to overlap, in some frames scattering from individual crystallites dominates. The lateral width of such crystallites was found by scanning to be generally within

the $2\ \mu\text{m}$ beam size. An almost single-crystallite pattern with the (001) and (002) reflections, recorded with an image plate, is shown in Fig. 3(a). Note an additional weak (001) reflection due to a second crystallite. From a two-dimensional Gaussian fit (Fig. 3b) the (001) peak width in the radial direction was determined to be $\Delta s = 0.017\ \text{nm}^{-1}$ (FWHM), which is similar to the average value of $\Delta s = 0.015\ \text{nm}^{-1}$ (FWHM) derived from the powder diffraction study (Huang *et al.*, 1993). The (001) reflection width has been attributed to particle-size broadening with an average particle size of 90 (5) nm (Huang *et al.*, 1993). Scanning electron microscopy on the powder sample used for the present study suggests a similar particle-size distribution.

Fig. 4 shows the positions of (001) reflections recorded in scanning mode which could be resolved. The reflections fall within two concentric rings, the width of which corresponds to $\Delta s = 0.017\ \text{nm}^{-1}$. The distribution reflects the sampling by the Ewald sphere of reciprocal lattice points of finite size (on account of the small particle size) corresponding to the different crystallites in the stationary sample.

Background correction was possible down to an s value of *ca* $0.1\ \text{nm}^{-1}$ ($d \simeq 10\ \text{nm}$). This should be compared with an ideal value of $s_{\text{min}} \simeq 0.025\ \text{nm}^{-1}$ ($d_{\text{max}} \simeq 40\ \text{nm}$), corresponding to the limits of the direct beam.

5. Conclusions

The present results suggest the possibility of performing low-angle scattering on organic samples with volumes in the range of $\geq 10^{-1} \mu\text{m}^3$ down to at least $s \simeq 0.1 \text{ nm}^{-1}$. A further reduction of s_{min} seems to be feasible. As compared with single-crystal Bragg–Fresnel optics (Snigirev *et al.*, 1993), a similar beam size has been reached in the present case but for a more limited s_{min} value. The interest in pursuing glass-capillary optics for low-angle scattering resides in the high monochromatic flux densities reached (Riekkel & Engström, 1995) which could be further increased by using a broader bandpass. Furthermore, such optics could be readily incorporated into collimation systems on diffractometers, thus providing an easy possibility for developing combined WAXS/SAXS instrumentation.

The authors thank P. Fratzl for the provision of the silver behenate sample.

References

- Bilderback, D. H., Thiel, D. J., Pahl, R. & Brister, K. E. (1994). *J. Synchrotron Rad.* **1**, 37–42.
- Engström, P. (1991). Thesis, Chalmers Tekniska Högskola, Sweden.
- Engström, P., Fiedler, S. & Riekkel, C. (1995). *Rev. Sci. Instrum.* **66**(2), 1348–1350.
- Engström, P., Riekkel, C. & Chanzy, H. (1995). *ESRF Newsl.* **24**, 8.
- Hammersley, A. P. (1995). *FIT2D*. Version 5.18. *Reference Manual*. Version 1.6. ESRF Internal Report, EXP/AH/95–01. ESRF, Grenoble, France.
- Hammersley, A. P., Svensson, S. O. & Thompson, A. (1994). *Nucl. Instrum. Methods*, **A346**, 312–321.
- Huang, T. C., Toraya, H., Blanton, T. N. & Wu, Y. (1993). *J. Appl. Cryst.* **26**, 180–184.
- Riekkel, C. & Engström, P. (1995) *Nucl. Instrum. Methods*, **B97**, 224–230.
- Snigirev, A., Snigireva, I., Riekkel, C., Miller, A., Wess, L. & Wess, T. (1993). *J. Phys. (Paris) Colloq.* **C8**, **3**, 443–446.
- Thiel, D. J., Stern, E. A., Bilderback, D. H. & Lewis, A. (1989). *Physica*, **B158**, 314–316.